Synthesis, Structure, and Optical-Limiting Properties of Heterobimetallic [M_3CuS_4] Cuboidal Clusters (M = Mo or W) with Terminal Phosphine Ligands

Marta Feliz,[†] Juan M. Garriga,[†] Rosa Llusar,*[,†] Santiago Uriel,[†] Mark G. Humphrey,[‡,§] Nigel T. Lucas,[‡] Marek Samoc,[||] and Barry Luther-Davies[||]

Departament de Ciències Experimentals, Universitat Jaume I, Campus de Riu Sec, P.O. Box 224, Castelló, Spain, Department of Chemistry, Australian National University, Canberra, ACT 0200, Australia, and Laser Physics Centre, Research School of Physical Sciences and Engineering, Australian National University, Canberra, ACT 0200, Australia

Received January 24, 2001

Cubane-type clusters of formula $[Mo_3CuS_4Cl_4(dmpe)_3](PF_6)$ (**4**), $[Mo_3CuS_4Br_4(dmpe)_3](PF_6)$ (**5**), and $[W_3CuS_4Br_4(dmpe)_3](PF_6)$ (**6**) have been prepared by reacting the incomplete cuboidal trimers $[Mo_3S_4Cl_3(dmpe)_3](PF_6)$ (**1**), $[Mo_3S_4Br_3(dmpe)_3](PF_6)$ (**2**), and $[W_3S_4Br_3(dmpe)_3](PF_6)$ (**3**), respectively, with CuX (X = Cl or Br) or the mononuclear copper complex $[Cu(CH_3CN)_4]^+$ in THF. The reaction takes place without global changes in the metal oxidation states, and compounds **4**−**6** with a $[M_3CuS_4]^{5+}$ core possess 16 e^- for metal−metal bonding. X-ray structural analysis of **4**−**6** revealed an effective C_{3v} symmetry for the M_3Cu unit with the M−M distances being statistically the same for M = Mo or W. However, the M−Cu distance is 0.04 and 0.1 Å longer than the M−M bond length for Mo and W, respectively. There is no significant structural rearrangement of the ligand−metal bonding in proceeding from $[M_3S_4X_3(dmpe)_3]^+$ to $[M_3CuS_4X_4(dmpe)_3]^+$. The cyclic voltammograms of the $[Mo_3CuS_4]$ cubane clusters show one quasi-reversible reduction process at $E_{1/2} = -0.31$ V for **4** and at $E_{1/2} = -0.23$ V for **5** and one irreversible reduction at −0.69 and −0.58 V for **4** and **5**, respectively. The tungsten cluster **6** shows a unique quasi-reversible reduction wave at $E_{1/2} = -0.71$ V. The incorporation of copper into the incomplete $[M_3S_4]$ cuboidal complexes produces a decrease of the reduction potential for both molybdenum and tungsten. Absorption spectra of **1**−**6** are broadly similar; replacing Mo by W in proceeding from **2** to **3** or from **5** to **6** and replacing Br by Cl in proceeding from **2** to **1** or from **5** to **4** results in a blue shift of the three UV−visible absorption bands. All six clusters exhibit optical limiting, as measured by the Z-scan technique at 523 nm using 40 ns pulses. The power-limiting mechanism remains obscure, but under the conditions employed, threshold-limiting fluence decreases on replacing W by Mo on proceeding from **3** to **2** or **6** to **5** and on proceeding from tetranuclear cluster (**4**−**6**) to trinuclear precursor (**1**−**3**, respectively). For all six clusters, values of the excited-state cross section σ_{eff} are larger than those of the corresponding ground-state cross section σ_0; i.e., all clusters are efficient optical limiters.

Introduction

Optical limiting is a phenomenon where the transmission through a material tends to saturate as the incident intensity increases; it is therefore attracting significant current attention as a means of optical device and eye protection, with both military (e.g. protection of personnel in the field) and laboratory applications (e.g. safety glasses for lasers that permit normal viewing at low light intensities). The optical-limiting merit of transition metal clusters has attracted much interest recently.[1−18] Metal clusters have several advantages as compared to other compounds traditionally investigated as potential third-order nonlinear optical (NLO) materials, such as semiconductors,

* To whom correspondence should be addressed. Fax: +34 964 728066. E-mail: llusar@exp.uji.es.

[†] Universitat Jaume I.

[‡] Department of Chemistry, Australian National University.

[§] To whom correspondence regarding the optical limiting should be addressed. Fax: +61 2 61250760. E-mail: Mark.Humphrey@anu.edu.au.

[||] Laser Physics Centre, Research School of Physical Sciences and Engineering, Australian National University.

(1) Hou, H.-W.; Xin, X.-Q.; Liu, J.; Chen, M.-Q.; Shu, S. *J. Chem. Soc., Dalton Trans.* **1994**, 3211.
(2) Shi, S.; Ji, W.; Lang, J. P.; Xin, X. Q. *J. Phys. Chem.* **1994**, *98*, 3570.
(3) Shi, S.; Ji, W.; Tang, S. H.; Lang, J. P.; Xin, X. Q. *J. Am. Chem. Soc.* **1994**, *116*, 3615.
(4) Ji, W.; Shi, S.; Du, H. J.; Ge, P.; Tang, S. H.; Xin, X. Q. *J. Phys. Chem.* **1995**, *99*, 17297.
(5) Long, D.-L.; Shi, S.; Xin, X.-Q.; Luo, B.-S.; Chen, L.-R.; Huang, X.-Y.; Kang, B.-S. *J. Chem. Soc., Dalton Trans.* **1996**, 2617.
(6) Hou, H.-W.; Xin, X.-Q.; Shi, S. *Coord. Chem. Rev.* **1996**, *153*, 25.
(7) Zeng, D.-X.; Ji, W.; Wong, W.-T.; Wong, W.-Y.; Xin, X. Q. *Inorg. Chim. Acta* **1998**, *279*, 172.
(8) Philip, R.; Kumar, G. R.; Mathur, P.; Ghosh, S. *Chem. Phys. Lett.* **1999**, *313*, 719.
(9) Hou, H.; Fan, Y.; Du, C.; Zhu, Y.; Wang, W.; Xin, X.; Low, M. K. M.; Ji, W.; Ang, H. G. *Chem. Commun.* **1999**, 647.
(10) Whittall, I. R.; McDonagh, A. M.; Humphrey, M. G.; Samoc, M. *Adv. Organomet. Chem.* **1999**, *43*, 349.
(11) Zhang, Q.-F.; Raj, S. S. S.; Fun, H.-K.; Xin, X.-Q. *Chem. Lett.* **1999**, 619.
(12) Zheng, H.-G.; Tan, W.-L.; Ji, W.; Leung, W.-H.; Williams, I. D.; Long, D.-L.; Huang, J.-S.; Xin, X.-Q. *Inorg. Chim. Acta* **1999**, *294*, 73.
(13) Tan, W.; Zheng, H.; Jin, Q.; Jin, G.; Ji, W.; Long, D.; Xin, X. *Polyhedron* **2000**, *19*, 1545.
(14) Song, Y.; Zhang, C.; Zhao, X.; Wang, Y.; Fang, G.; Jin, G.; Qu, S.; Wu, S.; Xin, X.; Ye, H. *Chem. Lett.* **2000**, 1076.
(15) Zhang, Q.-F.; Leung, W.-H.; Xin, X.-Q.; Fun, H.-K. *Inorg. Chem.* **2000**, *39*, 417.
(16) Zhang, C.; Song, Y.; Xu, Y.; Fun, H.; Fang, G.; Wang, Y.; Xin, X. *J. Chem. Soc., Dalton Trans.* **2000**, 2823.
(17) Zhang, Q.-F.; Xiong, Y.-N.; Lai, T.-S.; Ji, W.; Xin, X.-Q. *J. Phys. Chem. B* **2000**, *104*, 3446.
(18) Zhang, C.; Song, Y.; Jin, G.; Fang, G.; Wang, Y.; Raj, S. S. S.; Fun, H.-K.; Xin, X. *J. Chem. Soc., Dalton Trans.* **2000**, 1317.

10.1021/ic010098y CCC: $20.00
Published on Web 10/17/2001

organic polymers, carbon-based C_{60}, and mononuclear metallophthalocyanines, in the following aspects: (i) The constituent elements are generally heavier, introducing many more energy sublevels as compared to carbon-based molecules. (ii) The heavy atoms in the cluster can favor intersystem crossing mechanisms via spin−orbit coupling. (iii) The metal atoms and terminal ligands can be easily varied, yielding more versatility to the system. (iv) Coordination geometries and structure types can be explored to achieve desired NLO functions.

Strong optical limiting effects have been reported for sulfur- or selenium-containing clusters with a cubanelike structure and MM'_3S_3Br or $M_3M'Se_4$ (M = Mo, W; M′ = Cu, Ag) central units.[2,3,17] Cubane-type chalcogenide clusters have the advantage that their constituent metals are all triply bridged (μ_3) by chalcogenides. This coordination mode provides the central cluster unit with great stability, particularly toward light-induced fragmentation caused by the electronic transition between the skeletal bonding and antibonding orbitals. Our research interest has been focused on the use of rational synthetic routes for the preparation of cuboidal trinuclear and tetranuclear metal−chalcogenido clusters and the investigation of their potential applications, such as NLO properties. In this work we present the synthesis, structure, redox properties, and optical-limiting capability of cubane cationic compounds with phosphine terminal ligands, namely $[Mo_3CuS_4X_4(dmpe)_3]^+$ (X = Cl and Br) and $[W_3CuS_4Br_4(dmpe)_3]^+$. The structural, redox, and optical properties of these clusters are compared with those of their trinuclear precursors.

Experimental Section

Materials. The polymeric phases $Mo_3S_7Cl_4$, $Mo_3S_7Br_4$, and $W_3S_7Br_4$ were prepared by solid-state reactions according to literature methods.[19,20] The molecular triangular clusters $[Mo_3S_4Cl_3(dmpe)_3](PF_6)$ (**1**), $[Mo_3S_4Br_3(dmpe)_3](PF_6)$ (**2**), and $[W_3S_4Br_3(dmpe)_3](PF_6)$ (**3**) were synthesized by excision of the above polymeric phases following the procedure recently developed by us.[21] $[Cu(CH_3CN)_4](PF_6)$ was synthesized from commercial Cu_2O and HPF_6 in acetonitrile.[22] The remaining reactants were obtained from commercial sources and used as received. Solvents for synthesis and electrochemical measurements were dried and degassed by standard methods before use. Chromatographic work was performed on 60 Å silica gel columns.

Physical Measurements. Elemental analyses were carried out with a C. E. analyzer, model EA 1108. $^{31}P\{^1H\}$ NMR spectra were recorded in CH_3CN with a reference scale of 85% H_3PO_4. IR spectra were recorded on a Perkin-Elmer System 2000 FT-IR using KBr pellets. Cyclic voltammetry experiments were performed with an Echochemie Pgstat 20 electrochemical analyzer with a conventional three-electrode configuration consisting of platinum working and auxiliary electrodes and a Ag/AgCl reference electrode containing aqueous 3 M KCl. All measurements were carried out in acetone using tetra-*n*-butylammonium hexafluorophosphate (0.1 M) as supporting electrolyte. $E_{1/2}$ values were determined as $^1/_2(E_a + E_c)$, where E_a and E_c are the anodic and cathodic peak potentials, respectively. All potentials reported are not corrected for the junction potential. The $E_{1/2}$ value obtained for ferrocene under these experimental conditions is 0.50 V. Electrospray mass spectra were recorded on a Micromass Quattro LC instrument using nitrogen as drying and nebulizing gas.

Optical-Limiting Studies. Optical measurements of acetonitrile solutions were carried out in 1 mm thick glass cells. Linear optical spectra were obtained on a Cary 4 spectrophotometer over the spectral range 320−900 nm. The system for optical-limiting studies employed a Nd:YLF laser operating at the second harmonic wavelength of 523 nm, pulse length 40 ns, and repetition rate 20 Hz. The experiments were performed on solutions of concentrations ca. 5 mg mL^{-1}. The power-limiting curves were obtained by the open-aperture Z-scan technique.[23] The data were then converted into transmittance−fluence plots by assuming Gaussian character of the beam.

Syntheses. $[Mo_3CuS_4Cl_4(dmpe)_3](PF_6)$ (4). Method 1. To a solution of $[Mo_3S_4Cl_3(dmpe)_3](PF_6)$ (0.10 g, 0.09 mmol) and tetrabutylammonium chloride, (TBA)Cl (0.05 g, 0.18 mmol), in THF (40 mL) was added an excess of $[Cu(CH_3CN)_4](PF_6)$ (0.108 g, 0.29 mmol) under nitrogen. The color of the solution changed from green to brown immediately. After the reaction mixture was stirring for 24 h, a colloidal brown precipitate was formed, and it was separated from the solution by centrifugation and further decantation. The resulting solid was taken to dryness, redissolved in CH_2Cl_2, and adsorbed on a silica gel column. After washing of the column with acetone, elution with a KPF_6 solution in acetone (10 mg/mL) afforded a very concentrated brown solution. This solution was taken to dryness, redissolved in CH_2Cl_2, and filtered to eliminate the insoluble KCl or KPF_6 inorganic salts. The (TBA)Cl salt was separated from the solution by four consecutive water extractions (50:50). After drying of the organic solution with anhydrous $MgSO_4$, it was filtered and allowed to evaporate slowly in air to give 80 mg of an air-stable brown microcrystalline solid characterized as $[Mo_3CuS_4Cl_4(dmpe)_3](PF_6)$ (**4**) (yield: 73%).

Method 2. To a green solution of $[Mo_3S_4Cl_3(dmpe)_3](PF_6)$ (0.14 g, 0.13 mmol) in THF (40 mL) was added an excess of CuCl (0.046 g, 0.46 mmol) under nitrogen. The color of the solution turned brown after 1 h. After the reaction mixture was stirring for 24 h, a brown precipitate containing the desired cluster compound was obtained. This precipitate was separated from the solution in the same way as reported in method 1. This solid was redissolved in CH_2Cl_2, purified by silica gel column chromatography, and filtered to remove the inorganic salts. Finally, the resulting solution was allowed to evaporate slowly in air to give an air-stable brown solid (70 mg) characterized as $[Mo_3CuS_4Cl_4(dmpe)_3](PF_6)$ (**4**) (yield: 46%).

Anal. Calcd for $C_{18}H_{48}F_6P_7S_4Cl_4CuMo_3$: C, 17.77; H, 3.98. Found: C, 17.73; H, 4.11.

$^{31}P\{^1H\}$ NMR (δ, ppm): 25.20 (dd), 30.34 (dd) (AA′A″BB′B″ system).

IR (KBr, cm^{-1}): 1416 (s), 1289 (s), 1138 (s), 940 (s), 904 (s), 841 (s), 744 (m), 716 (m), 652 (m), 558 (s), 521 (w), 442 (w), 413 (w), 356 (w), 329 (w), 312 (w).

Electrospray MS (CH_2Cl_2, 60 V, *m*/*z*): 1073 (M^+).

$[Mo_3CuS_4Br_4(dmpe)_3](PF_6)$ (5). Method 1. This compound was prepared by following the first procedure described for **4** except that $[Mo_3S_4Br_3(dmpe)_3](PF_6)$ (0.11 g, 0.09 mmol) and (TBA)Br (0.057 g, 0.18 mmol) were used instead of $[Mo_3S_4Cl_3(dmpe)_3](PF_6)$ and (TBA)Cl, respectively. The air-stable brown product obtained (60 mg) was characterized as $[Mo_3CuS_4Br_4(dmpe)_3](PF_6)$ (**5**) (yield: 49%).

Method 2. Complex **5** was prepared by following the second method described for **4** but using CuBr (0.046 g, 0.32 mmol) and $[Mo_3S_4Br_3(dmpe)_3](PF_6)$ (0.1 g, 0.08 mmol) instead of the corresponding chloride derivatives. The air-stable brown product (40 mg) was characterized as compound **5** (yield: 36%).

Anal. Calcd for $C_{18}H_{48}F_6P_7S_4Br_4CuMo_3$: C, 15.50; H, 3.47. Found: C, 15.58; H, 3.54.

$^{31}P\{^1H\}$ NMR (δ, ppm): 19.71 (dd), 29.22 (dd) (AA′A″BB′B″ system).

IR (KBr, cm^{-1}): 1414 (s), 1285 (m), 1139 (m), 938 (s), 904 (s), 839 (s, P−F), 745 (w), 708 (w), 650 (w), 588 (s), 441 (w), 414 (w), 376 (w), 344 (w), 327 (w), 314 (w), 302 (w).

Electrospray MS (CH_2Cl_2, 50 V, *m*/*z*): 1250 (M^+).

$[W_3CuS_4Br_4(dmpe)_3](PF_6)$ (6). Method 1. This compound was prepared by following the first method described for **4** except that $[W_3S_4Br_3(dmpe)_3](PF_6)$ (0.11 g, 0.07 mmol) and (TBA)Br (0.055 g, 0.17 mmol) were used instead of $[Mo_3S_4Cl_3(dmpe)_3](PF_6)$ and (TBA)-

(19) Cotton, F. A.; Kibala, P. A.; Matusz, M.; McCaleb, C. S.; Sandor, R. B. W. *Inorg. Chem.* **1989**, *28*, 2623.
(20) Fedin, V. P.; Sokolov, M. N.; Gerasko, O. A.; Kolesov, B. A.; Fedorov, V. Y.; Mironov, A. V.; Yufit, D. S.; Slovohotov, Y. L.; Struchkov, Y. T. *Inorg. Chim. Acta* **1990**, *175*, 217.
(21) Estevan, F.; Feliz, M.; Llusar, R.; Mata, J. A.; Uriel, S. *Polyhedron* **2001**, *20*, 527.
(22) Kubas, G. J. *Inorg. Synth.* **1979**, *2*, 90.
(23) Sheik-Bahae, M.; Said, A. A.; Wei, T.; Hagan, D. J.; van Stryland, E. W. *IEEE J. Quantum Electron.* **1990**, *26*, 760.

Table 1. Crystallographic Data for $[Mo_3CuS_4Cl_4(dmpe)_3](PF_6)$ (**4**), $[Mo_3CuS_4Br_4(dmpe)_3](PF_6)$ (**5**), and $[W_3CuS_4Br_4(dmpe)_3](PF_6)$ (**6**)

param	**4**	**5**	**6**
empirical formula	$C_{18}H_{48}Mo_3CuCl_4S_4P_7F_6$	$C_{24}H_{48}Mo_3CuBr_4S_4P_7F_6$	$C_{25}H_{48}W_3CuBr_4S_4P_7F_6$
fw	1216.75	1466.65	1749.37
space group	$P2_1/n$	$P\bar{3}$	$P2_1/n$
a, Å	12.5998(5)	13.9148(7)	12.7906(6)
b, Å	15.7947(6)	13.9148(7)	23.5941(11)
c, Å	21.3968(9)	13.9454(10)	16.3734(7)
α, deg	90.0	90.0	90.0
β, deg	90.0360(10)	90.0	90.3590(10)
γ, deg	90.0	120.0	90.0
V, Å^3	4258.2(3)	2338.4(2)	4941.1(4)
Z	4	2	4
λ, Å	0.710 73	0.710 73	0.710 73
p_{calcd}, g cm^{-3}	1.898	2.083	2.342
T, K	293(2)	293(2)	293(2)
μ(Mo Kα), mm^{-1}	2.108	5.114	11.059
R1[a]	0.039	0.044	0.046
wR2[b]	0.094	0.099	0.105

[a] $R1 = \Sigma||F_0| - |F_c||/\Sigma F_0$. [b] $wR2 = [\Sigma[w(F_0^2 - F_c^2)^2]/\Sigma[w(F_0^2)^2]]^{1/2}$.

Cl, respectively. The air-stable green product obtained (70 mg) was characterized as $[W_3CuS_4Br_4(dmpe)_3](PF_6)$ (**6**) (yield: 58%).

Method 2. Complex **6** was prepared and purified using the second procedure described for **4** but using CuBr (0.03 g, 0.21 mmol) instead of CuCl and $[W_3S_4Br_3(dmpe)_3](PF_6)$ (0.075 g, 0.47 mmol) instead of the analogous cluster choride. The air-stable green product (30 mg) was characterized as compound **6** (yield: 37%).

Anal. Calcd for $C_{18}H_{48}F_6P_7S_4Cl_4CuW_3$: C, 13.04; H, 2.92. Found: C, 12.95; H, 2.77.

$^{31}P\{^1H\}$ NMR (δ, ppm): −2.56 (s), −2.37 (s).

IR (KBr, cm^{-1}): 1419 (s), 1288 (m), 1141 (m), 940 (s), 905(m), 840 (s, P−F), 746 (m), 710 (m), 650 (m), 558 (s, P−F), 441 (w), 420(w), 372 (w), 358 (w), 337 (w), 303 (m).

Electrospray MS (CH_2Cl_2, 75 V, m/z): 1514 (M^+), 1218 (M^+ − CuBr − dmpe).

X-ray Data Collection and Structure Refinement. Suitable crystals for X-ray studies for **4**−**6** were grown by slow diffusion of ether into sample solutions in dichloromethane. Air-stable crystals were mounted on the tip of a glass fiber with the use of epoxy cement. X-ray data were collected on a Bruker Smart CCD diffractometer using graphite-monochromated Mo Kα radiation (λ = 0.710 73 Å) with a nominal crystal to detector distance of 4.0 cm. A hemisphere of data was collected on the basis of three ω-scan runs (starting $\omega = -28°$) at values ϕ = 0, 90, and 180° with the detector at $2\theta = 28°$. At each of these runs, frames (606, 435, and 230, respectively) were collected at 0.3° intervals and 40, 40, and 60 s per frame for compounds **4**−**6**, respectively. The diffraction frames were integrated using the SAINT package and corrected for absorption with SADABS.[24,25] The crystal parameters and basic information relating data collection and structure refinement for compounds **4**−**6** are summarized in Table 1.

The structures were solved by direct methods and refined by the full-matrix least-squares method based on F^2 using the SHELXTL 5.10 software package. Structures **4** and **6** were successfully refined in the monoclinic space group $P2_1/n$ despite having all angles close to 90°. All attempts made to refine any of these structures in an orthorhombic space group as single or twin crystals have failed. Structure **5** could only be refined successfully in the hexagonal space group $P\bar{3}$ although the "*c*" cell parameter is very close to "*a*" and "*b*". In addition, compounds **4** and **6** are not isostructural despite the similarities in their cell parameters. The non-hydrogen cluster atoms of structures **4**−**6** were refined anisotropically; the positions of all hydrogen atoms were generated geometrically, assigned isotropic thermal parameters, and allowed to ride on their respective parent carbon atoms. The PF_6^- anions in structures **4** and **6** were refined anisotropically. Two independent PF_6^- groups were found in structure **5**, both in special positions, and consistent with a cluster/PF_6^- ratio of one as observed for the two other structures. One of the PF_6^- anions in structure **5** was refined anisotropically, the other being refined as a rigid group which rotates about the phosphorus atom with a fixed isotropic thermal parameter of 0.1 assigned to the fluorine atoms. After refinement of structures **5** and **6,** the most intense peaks, two and seven for **5** and **6**, respectively, could only be assigned to the solvent although we could not find a feasible model, and these peaks were included as carbon atoms in order to improve the overall phasing.

Scheme 1

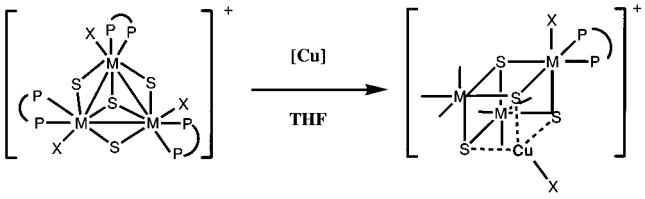

Results and Discussion

Synthesis. Methods for the preparation of cubane-type sulfido clusters can be categorized in two groups, namely spontaneous self-assembly and building-block synthesis.[26] In the second strategy, the individual units, sometimes referred to as "synthons", are used in the planned aggregation of a particular structure. In this work, we have prepared the cuboidal clusters of formula $[M_3CuS_4X_4(dmpe)_3]^+$ (M = Mo or W; X = Cl or Br) with $[M_3CuS_4]$ core units by following the second method (Scheme 1), using as building blocks the corresponding trinuclear sulfido clusters of general formula $[M_3S_4X_3(dmpe)_3]^+$, with $[M_3S_4]$ incomplete cuboidal units, and a mononuclear copper compound [Cu], $[Cu(CH_3CN)_4]^+$ or CuX.

The reaction of $[M_3S_4X_3(dmpe)_3]^+$ with an excess of $[Cu(CH_3CN)_4]^+$ in THF affords the desired product in ca. 40% yields for the molybdenum complexes and in 25% yield for the tungsten cluster. The source of the chloride or bromide attached to copper in the product is the corresponding cluster precursor, and as a consequence, it becomes a limiting reactant for this reaction. When the copper complex is substituted by the appropriate copper halide, CuCl or CuBr, to overcome the above limitation, the yields remain almost unchanged for the Mo compounds **4** and **5**, while the yield for the tungsten cluster **6** increases from 25 to 37 %. An improvement of the overall yield can be achieved when the reaction between the trinuclear cluster and the $[Cu(CH_3CN)_4]^+$ cation takes place in the

(24) *SAINT*, 5.0 ed.; Bruker Analytical X-ray Systems: Madison, WI, 1996.
(25) Sheldrich, G. M. *SADABS empirical absorption program*; University of Göttingen: Göttingen, Germany, 1996.
(26) Hidai, M.; Kuwata, S.; Mizobe, Y. *Acc. Chem. Res.* **2000**, *33*, 46.

presence of a soluble halide salt such as tetrabutylammonium chloride or bromide. In this last case the yields obtained are 73, 49, and 58% for **4**−**6**, respectively.

This strategy for the synthesis of cubane-type molybdenum and tungsten cluster sulfides was first reported for the aquo cation $[Mo_3FeS_4(H_2O)_{10}]^{4+}$ by Shibahara et al. in 1986.[27] Since then, 16 different heterometals have been added to the $[M_3S_4(H_2O)_9]^{4+}$ aquo ion for M = Mo and 6 for M = W.[28] In the case of copper, different oxidation states for the cluster unit have been identified, namely $[Mo_3CuS_4]^{4+}$ and $[Mo_3CuS_4]^{5+}$, although in both cases the copper oxidation state has been found to be one.[29,30] The $[Mo_3CuS_4]^{4+}$ core crystallizes as a double cubane-type cluster, while the $[M_3CuS_4]^{5+}$ core forms simple cubane structures for both molybdenum and tungsten.[31−33]

The extension of this chemistry to nonaqueous solvents is much more limited although the Cu system constitutes an exception. Xintao et al. have reported the synthesis of a series of clusters of general formula $[M_3CuS_4(dtp)_3(\mu_2\text{-}CH_3CO_2)L]$ with dtp = dithiophosphate and L = solvent, in which the most remarkable difference with the previously reported complexes, as well as with the complexes presented in this work, is the presence of a bridging carboxylate ligand between two of the group 6 metal atoms of the clusters.[34−36] Hegetschweiler et al. have also prepared in nonaqueous solvents the molybdenum cluster $[Mo_3CuBrS_4(tdci)_3]^{3+}$ (tdci = *cis*-1,3,5-tris(dimethylamino)inositol) with a simple cubane structure and a $[Mo_3CuS_4]^{4+}$ core.[37] In contrast with ours and Xintao's synthetic strategies, these authors use copper metal instead of a Cu(I) compound as starting material. The complexes reported in this work are the first examples of a cubane-type cluster with a $[M_3CuS_4]$ central unit with the molybdenum or tungsten atoms coordinated to phosphine ligands. This ligand environment provides the cluster core unit with enhanced stability, as inferred from electrospray mass spectrometry (ESI-MS) results. The main feature of the ESI spectra of these cubane complexes is the presence of an abundant molecular ion. When the ionization energy is increased, peaks due to the simultaneous loss of CuX plus one diphosphine, followed by the loss of a second diphosphine, are observed. This is indicative of a very robust central $[M_3CuS_4]$ unit, particularly when compared with the fragmentation pathway of the very stable trinuclear precursors for which successive loss of the diphosphine ligands is also observed.

Structure. All complexes **4**−**6** assume cubane-type structures as represented in Figure 1 for compound **4**. Compound **5** has a real C_3 axis defined by the sulfur atom S(1) and the copper atom, with a unique Mo−Mo distance of 2.7936(9) Å and a Mo−Cu distance of 2.8233(13) Å. Compounds **4** and **6** do not have crystallographically imposed C_3 symmetry; however, the small deviations in the intermetallic distances are indicative of an effective C_3 symmetry for these complexes, in agreement with the two different resonance signals observed in the ^{31}P NMR spectra. Table 2 lists an average of the most relevant bond distances for compounds **4**−**6** using the atom-numbering scheme defined in Figure 1, together with those reported for their trinuclear parent clusters.

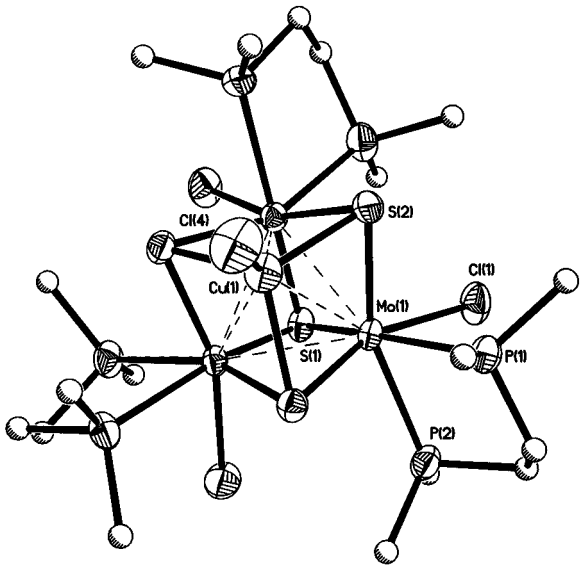

Figure 1. ORTEP diagram of **4** with 50% thermal ellipsoids and atom-numbering scheme.

The M−M distances within the M_3Cu core with an effective C_{3v} symmetry do not change significantly between molybdenum and tungsten. In contrast, the Mo−Cu bond distance is 0.04 Å longer than the Mo−Mo distance while the W−Cu bond length is 0.1 Å longer than the W−W distance. As a consequence, the W_3Cu unit is more distorted, by elongation along the C_3 axis.

There is no significant structural rearrangement of the ligand−metal bonding in proceeding from $[M_3S_4X_3(dmpe)_3]^+$ to $[M_3CuS_4X_4(dmpe)_3]^+$. Ignoring the metal−metal bonds, each molybdenum or tungsten atom is in a pseudooctahedral environment defined by three sulfur atoms, one S(1) and two S(2), one halide atom, and the chelating diphosphine. The coordination environment of copper is pseudotetrahedral. The addition of the Cu atom to the $[M_3S_4]$ incomplete cuboidal unit is coupled with a slight elongation of the M−M bond. The M−S(2) bonds that involve the sulfur atoms attached to the entering Cu atom are also slightly elongated. On the other hand, the M−S(1) bond distance, where S(1) is the sulfur atom which is triply bridged in the precursor, remains practically unchanged. There are two kinds of M−μ_3-S(2) bond distances, with the one approximately trans to the M−P bond being significantly longer (by 0.041, 0.033, and 0.034 Å for compounds **4**−**6**, respectively). The two types of M−P distances also differ by 0.054 Å for **4**, 0.053 Å for **5**, and 0.058 Å for **6**, with the one trans to the capping S(1) atom being shorter. These tendencies have also been observed for the trinuclear precursor complexes.[38,39] Table 3 compares the intermetallic bond distances for the compounds presented in this work with those of other representative $[M_3CuS_4]$ clusters reported in the literature.

These clusters have been classified into two groups, depending on the number of their cluster electrons. Compounds **4**−**6**

(27) Shibahara, T.; Akashi, H.; Kuroya, H. *J. Am. Chem. Soc.* **1986**, *108*, 1342.
(28) Hernández-Molina, R.; Sykes, A. G. *J. Chem. Soc., Dalton Trans.* **1999**, 3137.
(29) Nasreldin, M.; Li, Y.-J.; Frank, E. M.; Sykes, A. G. *Inorg. Chem.* **1994**, *33*, 4283.
(30) Miyamoto, R.; Kawata, S.; Iwaizumi, M.; Akashi, H.; Shibahara, T. *Inorg. Chem.* **1997**, *36*, 542.
(31) Shibahara, T.; Akashi, H.; Kuroya, H. *J. Am. Chem. Soc.* **1988**, *110*, 3313.
(32) Nasreldin, M.; Routledge, C. A.; Sykes, A. G. *J. Chem. Soc., Dalton Trans.* **1994**, 2809.
(33) Akashi, H.; Shibahara, T. *Inorg. Chim. Acta* **2000**, *300*−*302*, 572.
(34) Xintao, W.; Shaofeng, L.; Lianyong, Z.; Qiangjin, W.; Jiaxi, L. *Inorg. Chim. Acta* **1987**, *133*, 39.
(35) Xintao, W.; Huqiang, Z.; Yifan, Z.; Jiaxi, L. *J. Mol. Struct.* **1989**, *197*, 33.
(36) Huqiang, Z.; Yifan, Z.; Xintao, W.; Jiaxi, L. *Inorg. Chim. Acta* **1989**, *156*, 277.
(37) Hegetschweiler, K.; Wörh, M.; Meienberger, M. D.; Nesper, R.; Schmalle, H. W.; Hancock, R. D. *Inorg. Chim. Acta* **1996**, *250*, 35.
(38) Cotton, F. A.; Llusar, R. *Polyhedron* **1987**, *6*, 1741.
(39) Cotton, F. A.; Mandal, S. K. *Inorg. Chim. Acta* **1992**, *192*, 71.

Table 2. Selected Averaged Bond Distances (Å) for Compounds **4**−**6** and Their Trinuclear Precursors **1** and **3**

dist (Å)	$[Mo_3CuS_4Cl_4(dmpe)_3]^+$ (**4**)	$[Mo_3CuS_4Br_4(dmpe)_3]^+$ (**5**)	$[W_3CuS_4Br_4(dmpe)_3]^+$ (**6**)	dist (Å)	$[Mo_3S_4Cl_3(dmpe)_3]^+$ (**1**)[38]	$[W_3S_4Br_3(dmpe)_3]^+$ (**3**)[39]
M−M	2.782(1)	2.7935(11)	2.780[2]	M−M	2.766(4)	2.763[6]
M−Cu	2.823[8]	2.8227(16)	2.884[7]			
M−μ_3-S(1)	2.370[1]	2.353(3)	2.363[2]	M−μ_3-S(1)	2.360(9)	2.379[25]
M−μ_3-S(2)[a]	2.320[2]	2.325(2)	2.331[5]	M−μ_2-S(2)[c]	2.290(7)	2.271[42]
M−μ_3-S(2)[b]	2.361[2]	2.358(2)	2.365[5]	M−μ_2-S(2)[d]	2.336(7)	2.311[32]
Cu−μ_3-S(2)	2.305[2]	2.304(2)	2.320[13]			
M−X	2.473[13]	2.6203(12)	2.627[12]	M−X	2.473(7)	2.640[22]
M−P(1)	2.536[4]	2.552(2)	2.540[2]	M−P(1)	2.534(8)	2.509[37]
M−P(2)	2.590[5]	2.605(3)	2.598[3]	M−P(2)	2.605(8)	2.607[23]

[a] Mo−S−(Mo, Cu) trans distance to Mo-X bond. [b] Mo−S−(Mo, Cu) trans distance to Mo−P(2) bond. [c] Mo−μ_2-S trans distance to Mo−X bond. [d] Mo−μ_2-S trans distance to Mo−P(2) bond.

Table 3. Comparison of Intermetallic Bond Lengths for $[M_3CuS_4]$ Cubane Clusters

		M−M dist (Å)			M−Cu dist (Å)		
	compd	max	min	av	max	min	av
16 e	$[Mo_3CuS_4(dtp)_3I(\mu_2\text{-}CH_3COO)(dmf)]$	2.770(2)	2.679(2)	2.732[47]	2.807(3)	2.885(3)	2.849[39]
	$[Mo_3CuS_4Cl(Hnta)_3](NH_4)\cdot 3H_2O$	2.778(1)	2.778(1)	2.778(1)	2.838(2)	2.838(2)	2.838(2)
	$[Mo_3CuS_4Cl_4(dmpe)_3]PF6$ (**4**)	2.7835(6)	2.7815(6)	2.782[1]	2.8250(8)	2.8204(8)	2.823[8]
	$[Mo_3CuS_4Br_4(dmpe)_3]PF6$ (**5**)	2.7935(11)	2.7935(11)	2.7935(11)	2.8227(16)	2.8227(16)	2.8227[16]
	$[W_3CuS_4(dtp)_3I(\mu_2\text{-}CH_3COO)(py)]$	2.7668(3)	2.6872(4)	2.737[43]	2.960(1)	2.8406(9)	2.910[62]
	$[W_3CuS_4Br_4(dmpe)_3]PF_6$ (**6**)	2.7816(8)	2.7784(8)	2.780[2]	2.8882(18)	2.876(2)	2.884[7]
17 e	$[Mo_3CuS_4Br(tdci)_3]Br_3$	2.838(2)	2.822(2)	2.832[8]	2.924(2)	2.902(2)	2.916[12]
	$[(H_2O)_9Mo_3S_4CuCuS_4Mo_3(H_2O)_9](pts)_8$	2.738(2)	2.722(2)	2.730[8]	2.952(2)	2.778(2)	2.886[94]

with a $[M_3CuS_4]^{5+}$ core possess 16 e$^-$ for metal−metal bonding. The Mo−Mo and Mo−Cu bond lengths in **4** and **5** show little differences compared to the corresponding distances in the 16 e$^-$ anionic cluster $[Mo_3CuS_4Cl(Hnta)_3]^{2-}$ (H_3nta = nitrilotriacetic acid).[33] The other $[M_3CuS_4]^{5+}$ complexes structurally characterized with 16 e$^-$ correspond to clusters with formula $[M_3CuS_4(dtp)_3(\mu_2\text{-}CH_3CO_2)L]$ (dtp = dithiophosphate and L = solvent) and a carboxylate ligand bridging two molybdenum or tungsten atoms causing a shortening of this metal−metal bond distance.[34,36] Although the presence of the bridging carboxylate excludes direct comparison with compounds **4**−**6**, it is possible to comment on trends. All M−M distances in the clusters $[M_3CuS_4(dtp)_3(\mu_2\text{-}CH_3CO_2)L]$ are shorter than those observed in complexes **4** and **5** for M = Mo and **6** for M = W. This shortening of the M−M is accompanied by a lengthening of the M−Cu bond distance. Compounds with $[M_3CuS_4]^{4+}$ cores and 17 e$^-$ for metal−metal bond formation have only been structurally characterized for molybdenum, two structure types, namely isolated cubane and double cubane, being identified.[31,37] In all cases, the Mo−Cu distances are longer than those observed for the 16 e$^-$ clusters. MO calculations on isolated $[Mo_3CuS_4]$ complexes suggest that the extra electron in the 17 e$^-$ cluster occupies an antibonding Mo−Mo and Mo−Cu orbital, explaining the longer Mo−Mo and Mo−Cu distances observed for $[Mo_3CuS_4Br(tdci)_3]^{3+}$ (tdci = *cis*-1,3,5-trideoxy-1,3,5-tris(dimethylamino)inositol).[30,40]

Redox Properties. The existence of clusters with different electron populations suggests some degree of redox behavior for these compounds. We have investigated this possibility by cyclic voltammetry, the redox properties of these cubane clusters being compared with those of their trinuclear precursors. Figure 2 shows the cyclic voltammogram for $[Mo_3CuS_4Cl_4(dmpe)_3](PF_6)$ (**4**) and its precursor $[Mo_3S_4Cl_3(dmpe)_3](PF_6)$ (**1**).

For the molybdenum cubane clusters **4** and **5**, the cyclic voltammogram shows two waves within the potential range investigated (between 0 and −0.9 V), which correspond to one quasi-reversible reduction process at $E_{1/2} = -0.31$ V ($\Delta E =$ 0.06 V) for **4** and at $E_{1/2} = -0.23$ V ($\Delta E = 0.06$ V) for **5**, and one irreversible reduction at −0.69 V and −0.58 V for **4** and **5,** respectively. The corresponding molybdenum trinuclear precursors show a unique quasi- reversible reduction wave (Figure 2) within the potential range investigated at −0.63 V for **1** and at −0.50 V for **2**, attributed to the two-electron reduction $Mo^{IV}_3 \leftrightarrow Mo^{III}_2Mo^{IV}$.[21] In these trinuclear complexes this two-electron process can be seen as two one-electron reduction waves $Mo^{IV}_3 \leftrightarrow Mo^{III}Mo^{IV}_2 \leftrightarrow Mo^{III}_2Mo^{IV}$ under certain experimental conditions (solvent, counterion, etc.).[41]

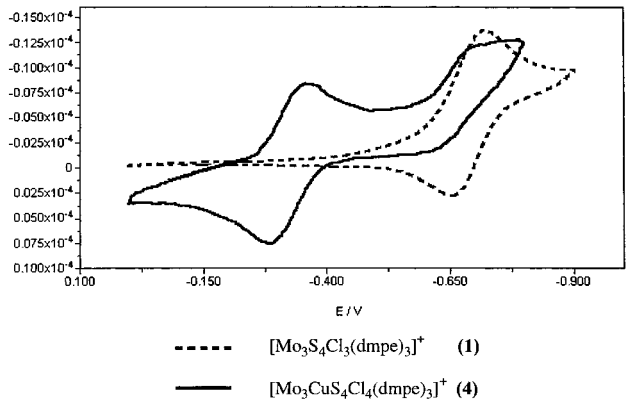

Figure 2. Cyclic voltammogram for compounds **1** and **4** in acetone. Scan rate: 500 mV s^{-1}.

The first quasi-reversible wave in the voltammogram of the 16 e$^-$ clusters **4** and **5** can be tentatively assigned to a one-electron process, affording the 17 e$^-$ cluster. EPR analysis and theoretical molecular orbital calculations on the 17 e$^-$ aquo cluster $[Mo_3CuS_4(H_2O)_{10}]^{4+}$ indicate that the three molybdenum ions are not equivalent to each other but rather formally approximate to Mo^{III}, Mo^{IV}, and Mo^{IV} and that there is little spin density on copper consistent with a formal oxidation state of Cu^{I}.[30] As a consequence, the first reduction wave for **4** and **5** can be attributed to the process $Mo^{IV}_3Cu^{I} \leftrightarrow Mo^{III}Mo^{IV}_2Cu^{I}$.

(40) Bahn, C. S.; Tan, A.; Harris, S. *Inorg. Chem.* **1998**, *37*, 2770.

(41) Cotton, F. A.; Llusar, R.; Eagle, C. T. *J. Am. Chem. Soc.* **1989**, *111*, 4332.

Table 4. Linear Optical and Optical-Limiting Data for Clusters **1**−**6**

cluster	optical abs λ, nm (ϵ, 10^3 dm^3 mol^{-1} cm^{-1})			ϵ_{523} (dm^3 mol^{-1} cm^{-1})	$F_{15\%}$ (J cm^2)[a]	cross section ($\times 10^{-18}$ cm^2)	
	λ_1 (ϵ_1)	λ_2 (ϵ_2)	λ_3 (ϵ_3)			ground state, σ_0	excited state, σ_{eff}
$[Mo_3S_4Cl_3(dmpe)_3]PF_6$ (**1**)	341 (6.0)	398 (4.6)	634 (0.42)	28	0.22	1.1	6.3
$[Mo_3S_4Br_3(dmpe)_3]PF_6$ (**2**)	353 (5.5)	410 (sh, 4.0)	642 (0.37)	30	0.14	1.1	6.8
$[W_3S_4Br_3(dmpe)_3]PF_6$ (**3**)	317 (sh, 13)	348 (sh, 8.1)	583 (0.71)	39	0.40	1.1	5.8
$[Mo_3CuS_4Cl_4(dmpe)_3]PF_6$ (**4**)	364 (sh, 5.4)	493 (2.4)	649 (sh, 0.42)	180	0.25	6.8	8.2
$[Mo_3CuS_4Br_4(dmpe)_3]PF_6$ (**5**)	381 (sh, 4.5)	499 (2.0)	661 (sh, 0.37)	164	0.45	6.3	7.0
$[W_3CuS_4Br_4(dmpe)_3]PF_6$ (**6**)	348 (sh, 5.2)	435 (1.6)	594 (0.38)	26	0.50	1.0	6.0

[a] $F_{15\%}$ is defined as the incident fluence needed to reduce the transmittance through the sample by 15%.

The second irreversible reduction can then be assigned to the one-electron process $Mo^{III}Mo^{IV}_2Cu^I \rightarrow Mo^{III}_2Mo^{IV}Cu^I$, because the redox potentials are very close to those observed for the two-electron reduction ($Mo^{IV}_3 \leftrightarrow Mo^{III}_2Mo^{IV}$) in the trinuclear parent precursors, as can be seen in Figure 2. We can conclude that the two-electron reduction process observed for **1** and **2** is split into two one-electron reductions when copper is incorporated into the trinuclear [Mo_3] cluster to afford compounds **4** and **5**, with the resulting [Mo_3Cu] cubane clusters easier to reduce that the parent trimers. In the case of the tungsten cluster $[W_3CuS_4Br_4(dmpe)_3](PF_6)$ (**6**), we observed a unique quasi-reversible reduction wave at $E_{1/2} = -0.71$ V ($\Delta E = 0.07$ V), while the parent $[W_3S_4Br_3(dmpe)_3](PF_6)$ (**3**) complex shows a quasi-reversible reduction wave at $E_{1/2} = -1.01$ V; this corresponds to an anodic shift of the redox potential of ca. 0.3 V upon copper incorporation, similar to that observed for the molybdenum clusters.

The electrochemical behavior observed for the [M_3Cu] cubane clusters differs from that observed for the $[Mo_3FeS_4]^{4+}$ and $[Mo_3NiS_4]^{4+}$ aquo clusters. In the latter case, the incorporation of Fe or Ni into the $[Mo_3S_4]^{4+}$ aquo ion corresponds to a reduction of the trinuclear cluster, the resulting $[Mo_3FeS_4]^{4+}$ and $[Mo_3NiS_4]^{4+}$ complexes being ca. 0.45 V more difficult to reduce than the precursor aquo trimer.[42] In these cubane clusters the formal oxidation state of the metals would be more adequately expressed as $Mo^{IV}Mo^{III}_2Fe^{II}$ or $Mo^{IV}Mo^{III}_2Ni^{II}$, although we are aware of the extreme difficulty of assigning formal oxidation states to metal atoms involved in delocalized cluster bonding, as pointed out by Harris et al.[40] These authors conclude, on the basis of electronic structure calculations, that it is not appropriate to describe the Ni atom as oxidized in these clusters while the relatively high frequencies observed for the carbonyl ligand attached to Ni in these complexes had previously led other researchers to suggest that Ni is oxidized upon formation of the cubane clusters.[43] When main group metals, e.g. gallium, are incorporated into the $[Mo_3S_4]^{4+}$ aquo ion, the observed electrochemical properties are consistent with the formulation $Mo^{IV}Mo^{III}_2Ga^{III}$, and the resulting complex shows no Mo−Ga bond.[44] In this case the absence of a delocalized bond results in a more applicable assignment of the formal oxidation state of the metal. The [M_3S_4Cu] system constitutes the only example in which the incorporation of a second metal into the trinuclear parent complex produces a decrease of the reduction potential, but detailed research will be required to confirm the proposed mechanism.

Optical-Limiting Properties. The linear and nonlinear optical properties of the new clusters have been assessed, together with those of the precursor clusters. Linear optical spectra for complexes **1**−**3** are displayed in Figure 3 and for complexes **4**−**6** are shown in Figure 4. Important spectral data for all six clusters are listed in Table 4.

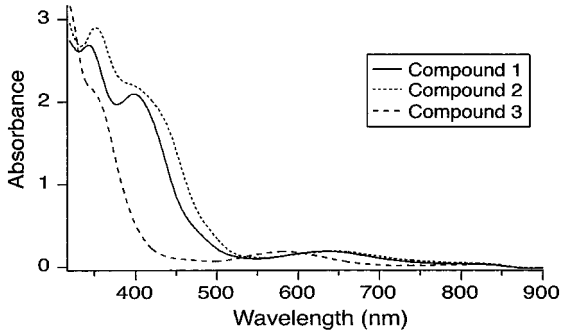

Figure 3. Linear optical spectra for complexes **1**−**3**.

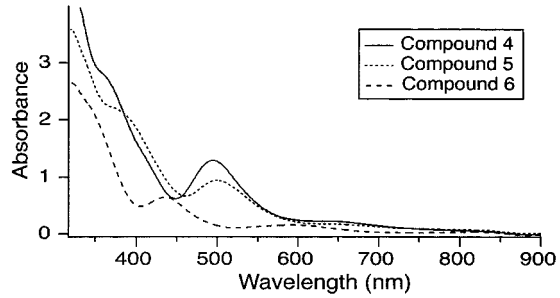

Figure 4. Linear optical spectra for complexes **4**−**6**.

The UV−visible spectra of clusters **1** and **2** contain intense bands at highest energy (λ_1, ca. 350 nm), less intense bands at lower energy (λ_2, ca. 400 nm), and weak bands at lowest energy (λ_3, ca. 640 nm). Replacing Mo by W in proceeding from **2** to **3** results in a 35−60 nm blue shift of all bands. We have not attempted to assign these transitions but note that the significant blue shift on replacing lighter by heavier metal suggests metal involvement in all three transitions. The effect of halide replacement on optical spectra is smaller, but constant, namely a blue shift in all three bands on replacing Br by Cl in proceeding from **2** to **1**. The UV−visible spectra of clusters **4**−**6** reveal similar trends to those seen with **1**−**3**: bands blue-shift on replacing Br by Cl and Mo by W. Introduction of Cu in proceeding from **1**, **2**, or **3** to **4**, **5**, or **6**, respectively, results in a significant red-shift in the absorption maximum. All six clusters contain broad low-intensity absorptions through the visible region, suggestive of potential as broad-band optical limiters.

Relevant data for optical limiting merit are collected in Table 4; all six clusters absorb weakly at the measurement wavelength of 523 nm. Optical limiting in the current clusters has been assessed using the Z-scan technique. Closed-aperture Z-scan is usually used to derive the nonlinear refractive index intensity coefficient n_2 by examining self-focusing or self-defocusing phenomena.[10] To determine the nonlinear absorption properties,

(42) Shibahara, T.; Sakane, G.; Naruse, Y.; Taya, K.; Akashi, H.; Ichimura, A.; Adachi, H. *Bull. Chem. Soc. Jpn.* **1995**, *68*, 2769.
(43) Shibahara, T.; Mochida, S.; Sakane, G. *Chem. Lett.* **1993**, *32*, 89.
(44) Shibahara, T.; Kobayashi, S.; Tsuji, N.; Sakane, G.; Fukuhara, M. *Inorg. Chem.* **1997**, *36*, 1702.

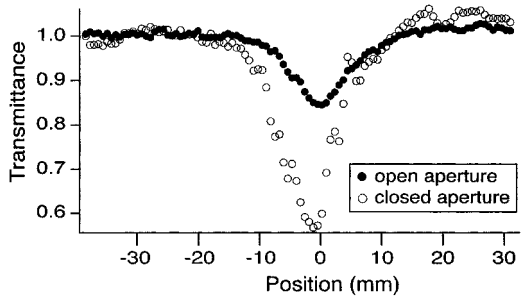

Figure 5. Open- and closed-aperture Z-scan plot for $[Mo_3S_4Cl_3(dmpe)_3]PF_6$ (**1**).

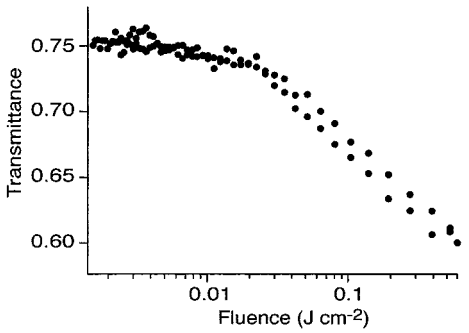

Figure 6. Optical-limiting behavior of $[Mo_3S_4Cl_3(dmpe)_3]PF_6$ (**1**).

the total transmission through a sample can be monitored by employing open-aperture Z-scan. Open- and closed-aperture Z-scan plots for an indicative cluster (**1**) are displayed in Figure 5. The major problem with nanosecond, nontime-resolved measurements (such as these Z-scan studies) is that the power-limiting mechanism remains obscure. In the present case, the closed aperture Z-scans reveal negative refractive, probably thermal, nonlinearity. It is therefore likely that a contribution to, and possibly the major part of, the effect originates from thermal processes which could be of several different mechanisms.

Transmission vs fluence (energy of laser/unit area) plots were generated, a representative plot (that of **1**) being shown in Figure 6. For comparative purposes, a threshold limiting fluence $F_{15\%}$ (defined as the incident fluence needed to reduce the transmittance through the sample by 15%) has been used to assess relative optical limiting merit of these clusters, the results being tabulated in Table 4. In general, threshold limiting fluence $F_{15\%}$ decreases on replacing W by Mo, and on proceeding from a tetranuclear cluster to trinuclear precursor cluster, but a full quantitative comparison between the data is not possible since the solutions have different absorptivities at the wavelength of 523 nm. There are few related structure−optical-limiting activity studies extant. Studies on related cubane clusters $WM_3(\mu_3\text{-}Br)(\mu_3\text{-}S)_3Br_3$ revealed a decrease in threshold limiting fluence on proceeding from M = Cu to M = Ag, but differences in laser beam parameters and other experimental variables are such that comparison of data between laboratories is not warranted.[2]

Assuming a simple three-state reverse saturable absorption model and using literature expressions, effective cross sections of the dominant excited states can be calculated.[45] The energy transmittance (with a Gaussian beam) is given by

$$T = (1 - R)^2 \frac{\exp(-\alpha_0 L)}{q} \ln(1 + q)$$

where

$$q = (1 - R)[1 - \exp(-\alpha_0 L)]\delta_{\text{eff}} F_0 / 2F_s$$

and R is the reflection coefficient, α_0 is the low power absorption coefficient, F_0 is the fluence, and F_s is the saturation fluence defined as

$$F_s = \frac{\hbar\omega}{\sigma_0}$$

and

$$\delta_{\text{eff}} = \frac{\sigma_{\text{eff}} - \sigma_0}{\sigma_0}$$

The effective excited-state cross section should only be considered a measure of the power-limiting ability of the substance under the given experimental conditions; it may contain contributions from several different excited states with different properties (e.g. from both a singlet and a triplet state). Values of excited-state cross-section σ_{eff} for clusters **1**−**6** are given in Table 4; they are larger than those of the corresponding ground-state cross-section σ_0; i.e., all clusters are efficient optical limiters.

The optical-limiting properties of a large number of clusters have been assessed, almost all examples being by experiments employing nanosecond pulses; as was mentioned above, comparisons of literature data with the present data, to extract structure−property relationships, are not warranted.[1−18,46] The present data are suggestive of replacement of W by Mo in these clusters resulting in an increase in σ_{eff}, but the values of σ_{eff} derived in these experiments are quite similar for all the clusters, suggesting a common power-limiting mechanism, possibly resulting from a purely thermal process. We are not able to comment further at present; the evaluation of the optical power-limiting mechanism requires picosecond time-resolved experiments.

Conclusions

Reaction of the incomplete cuboidal clusters $[M_3S_4X_3(dmpe)_3]^+$ (M = Mo, W; X = Cl, Br) with CuX or $[Cu(CH_3CN)_4]^+$ constitutes a rational "building-block" synthetic route to the cubane compounds of formula $[M_3CuS_4X_3(dmpe)_3]^+$. The copper incorporation into these trinuclear complexes results in a cathodic shift of the redox potential. The trinuclear and tetranuclear clusters are all efficient optical limiters ($\sigma_{\text{eff}} > \sigma_0$), with threshold-limiting fluence decreasing on proceeding from tetranuclear cluster to trinuclear precursor and from W-containing to Mo-containing analogue.

Acknowledgment. This work was supported by the Spanish Dirección General de Enseñanza Superior e Investigación Científica (DGESIC, research projects PB98-1044 and 1FD1997-1765-C03-02) and Fundació Caixa Castelló-UJI (research project P1B98-07). Thanks are also extended to the Servei Central d'Instrumentació Científica (SCIC) of the University Jaume I for providing us with mass spectrometry, nuclear resonance, and X-ray facilities. M.G.H. thanks the Australian Research Council for a Senior Research Fellowship. N.T.L. was an Australian Postgraduate Award recipient.

Supporting Information Available: X-ray crystallographic files in CIF format for complexes **4**−**6**. This material is available free of charge via the Internet at http://pubs.acs.org.

IC010098Y

(45) Sutherland, R. L. *Handbook of Nonlinear Optics*; Marcel Dekker: New York, 1996.
(46) Shi, S. *Optoelectronic Properties of Inorganic Compounds*; Roundhill, D. M., Fackler, J. P., Jr., Eds.; Plenum: New York, 1999; p 55.